FILTERING OF ARTIFACTS AND PAVEMENT SEGMENTATION FROM MOBILE LIDAR DATA

Jorge Hernández and Beatriz Marcotegui

Mines ParisTech
CMM- Centre de morphologie mathématique
Mathématiques et Systèmes
35 rue St Honoré 77305-Fontainebleau-Cedex, France
{ hernandez,marcotegui }@cmm.ensmp.fr

Commission III/2

KEY WORDS: LIDAR, point cloud, filtering ground data, segmentation ground data, mathematical morphology

ABSTRACT:

This paper presents an automatic method for filtering and segmenting 3D point clouds acquired from mobile LIDAR systems. Our approach exploits 3D information by using range images and several morphological operators. Firstly, a detection of artifacts is carried out in order to filter point clouds. The artifact detection is based on a Top-Hat of hole filling algorithm. Secondly, ground segmentation extracts the contour between pavements and roads. The method uses a quasi-flat zone algorithm and a region adjacency graph representation. Edges are evaluated with the local height difference along the corresponding boundary. Finally, edges with a value compatible with the pavement/road difference (about $14[cm]$) are selected. Preliminary results demonstrate the ability of this approach to automatically filter artifacts and segment pavements from 3D data.

1 INTRODUCTION

3D urban environment modeling becomes a fundamental part in a growing number of geo-applications as Google Earth, Microsoft Virtual Earth, IGN - Geoportail 3D, etc. The main approaches to model cities are based on coarse modeling, for instance: polyhedral representation, main walls, roof planes and ground planes. In recent years the laser telemetry has been gradually integrated on board systems to digitize the 3D geometry of natural and urban environments. The interpretation of 3D point clouds is one of the essential tasks in the urban modeling process. This interpretation consists in separating building façades, pavements, roads, artifacts (pedestrians, cars, trees, etc), and all elements which belong to urban scenes.

Several approaches are focused on façade modeling and urban scene segmentation. Automatic planar segmentation approaches from 3D façade data are presented in (Dold and Brenner, 2006, Stamos et al., 2006, Becker and Haala, 2007, Boulaassal et al., 2007). Region growing algorithms are used to extract planar surfaces (Dold and Brenner, 2006, Stamos et al., 2006) and planar approximation is carried out using RANSAC paradigm (Becker and Haala, 2007, Boulaassal et al., 2007). Madhavan and Hong (Madhavan and Hong, 2004) detect and recognize buildings from LIDAR data. Also, (Goulette et al., 2007) presents a segmentation based on profiles of points, for the following elements in the scene: ground (road and pavement), façades and trees. Nevertheless, those segmentation approaches are performed only on data acquired by their own acquisition systems.

To construct the complete city model, we need a ground model which could be combined with a model of buildings, improving the visual realism of synthetic scenes (Zhou and Neumann, 2008, Rottensteiner, 2003, Brostow et al., 2008). This work is focused on filtering of artifacts at the ground level and pavement segmentation, facilitating the urban modeling process, especially for façades and ground. A diagram illustrating the main steps

of our methods is shown in Figure 1. Each step will be further described through this paper.
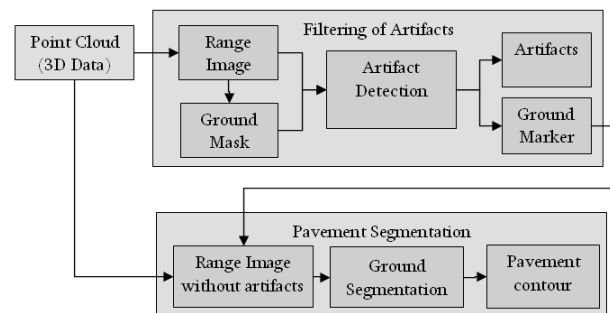

Figure 1: Main steps of our methods

Our research is developed in the framework of Cap Digital Business Cluster TerraNumerica project. This project aims to develop a production and exploitation platform, by allowing the definition and visualization of synthetic urban environments. The platform aims to increase productivity and realism of urban modeling.

The paper is organized as follows. Firstly, a 3D point cloud projection to a range image is presented in Section 2.3. Then, we detect and filter artifacts in order to clean up ground data (Section 3). In Section 4, a pavement segmentation is carried out. Finally, conclusions and our future work are drawn in Section 5.

2 3D DATA

2.1 Mobile Mapping Systems (MMS)

In this paper, 3D point clouds acquired by two different mobile mapping systems are used in order to test the proposed methods. These systems are LARA3D and Stereopolis. LARA3D MMS

was developed at CAOR/Mines ParisTech Lab-Research[1]. It consists in two perception sensors, a laser range finder and a camera equipped with a wide-angle fisheye lens, equipped with geo-localization sensors (GPS, IMU, odometers) (Brun et al., 2007). The range scanner covers an area of $270°$, by acquiring both sides of streets, the ground (pavement and road) and building top data. Stereopolis MMS, developed at MATIS laboratory of IGN[2], consists of a mobile platform with 16 full HD cameras, two laser sensors and geo-referencing devices. The laser sensors have a $80°$ field of view. They are facing the same side of the street at $90°$ and $45°$ degrees to façades. Depending on the distance from sensors to the façade, this system scans ground and building top data.

The point clouds of both systems are profiles distributed along the driving direction. Hence, the distance between two consecutive profiles depends on the vehicle speed and the sensor frequency. For Lara3D, the spacing is approximately $20 - 50[cm]$ and for Sterepolis, approximately $5 - 20[cm]$.

2.2 Database

3D Data correspond to approximately 2 street kilometers (30 city blocks) of the 5th Paris district. Figure 2(a) shows an example of an urban scene. As we can see, several objects, as parked cars, pedestrians and lamppost, produce occlusions in 3D data acquisition and disturbing the ground segmentation.
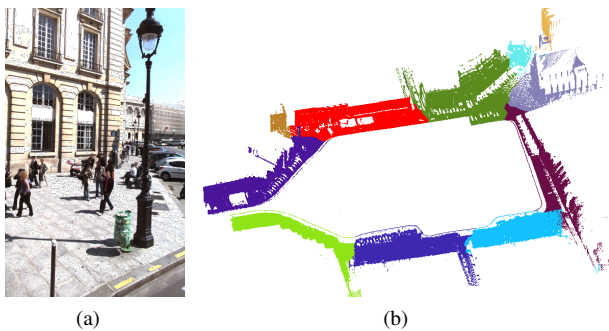

(a)   (b)

Figure 2: **(a)** Test zone image. **(b)** City blocks of *Place du Panthéon*

Besides, a pavement generally surrounds a city block. Thus, each city block is then processed separately. In order to segment point clouds into city blocks, the method described in (Hernández and Marcotegui, 2009) is used. An example of several city blocks is shown in Figure 2(b).

2.3 Range Image

We propose to exploit 3D data using a range image. The image is generated by projecting 3D points onto a plane using a " virtual " camera. The camera is placed on the plane with normal vector $\overrightarrow{n} = (0, 0, 1)$ through point $(0, 0, z_{min})$, i.e. parallel to plane XY and positioned on the lowest value of z coordinate. The image coordinates (u, v) are defined by a parametric function related to the camera. The range image is a representation of 3D information where the pixel intensity is a function of the measured distance between 3D points and the camera plane. If several points are projected on the same image coordinates, Z-buffer algorithm (Foley et al., 1995) is used to determine which distance is stored.

---

[1] caor.ensmp.fr/french/recherche/rvra/3Dscanner.php
[2] recherche.ign.fr/labos/matis/accueilMATIS.php

Range images are a $\mathbf{R}^3 \rightarrow \mathbf{N}^2$ projection. In order to avoid sampling problems, their dimensions should be chosen carefully. If they are too small, there will be an important information loss. Otherwise if they are too large, pixel connectivity (required by our method) is not ensured. Hence, the ideal choice of dimensions is $1 : 1$ i.e. a pixel by each 3D point in the camera plane. In our case, point clouds have a resolution of approximately $20[cm]$, and for this reason the selected resolution should be close to $5[pix/m]$.

3 FILTERING OF ARTIFACTS

Firstly, we filter artifacts using the method described in (Hernández and Marcotegui, 2009). Artifacts are all elements, static or mobiles, different from buildings and ground (pavement and road) data.

The method for artifact detection is based on hole filling algorithm (Soille and Gratin, 1994). The holes of an image correspond to sets of pixels whose minima are not connected to the image border (Soille, 2003). The algorithm consists in removing all minima which are not connected to the border by using the morphological reconstruction by erosion (Eq. 1). The image marker (mk) is set to the image maximum value everywhere, except along its border (Eq. 2).

$$\text{Fill}(f) = R_f^\varepsilon(mk) \qquad (1)$$

where,

$$mk = \begin{cases} f_p & \text{if } p \text{ lies on the border} \\ \max(f) & \text{otherwise} \end{cases} \qquad (2)$$

The method consists of several steps : firstly, a raw ground mask estimation is performed, using a quasi-flat zone algorithm. Secondly, a hole filling algorithm reduces several shadows (missing data produced by occlusions) and filters noise (concavities) on top of artifacts. Finally, assuming that artifacts are placed on the ground, they can be seen as humps. Hence, inverting the range image, those humps become new holes (concavities) to be filled. Then, the artifacts are detected by a hole filling top-hat, i.e. the difference between the inverted range image and the filled image. A threshold of $10[cm]$ is applied to the Top-Hat result in order to eliminate structures produced by ground roughness and noisy surfaces. The method allows to handle sloping streets because they are linked to the border. These steps are summarized in Figure 3.

Figure 4(a) shows a segmentation result, where 3D points are labelled as façade, artifact or ground. From the ground mask, we select all points that belong to the ground (excluding the artifacts). These points constitute a ground marker (Figure 4(b)).

4 PAVEMENT SEGMENTATION

In order to model realistic street level scenes, a pavement segmentation is required. We propose an automatic pavement segmentation, once the artifacts are eliminated from ground data. The range image used in the previous section has several defects, due to the ground points occluded by artifacts (for example points under a tree). Figure 5(a) shows an example, where all points under the tree are missing. To recover these points we reproject the ground marker onto the point cloud. We estimate a plane from the selected points. All points whose distance to the estimated plane is smaller than the mean estimation error are added to the

Figure 3: Diagram of artifact detection method.
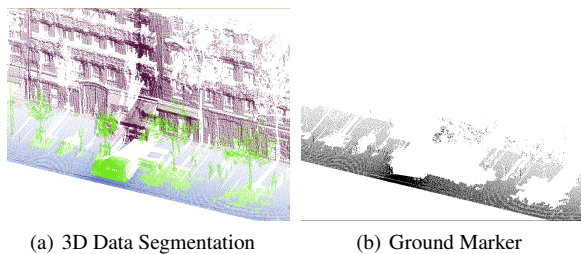

(a) 3D Data Segmentation   (b) Ground Marker

Figure 4: **(a)** 3D data segmentation: façade in violet, ground in blue and artifacts in green **(b)** Elimination of artifacts from ground data
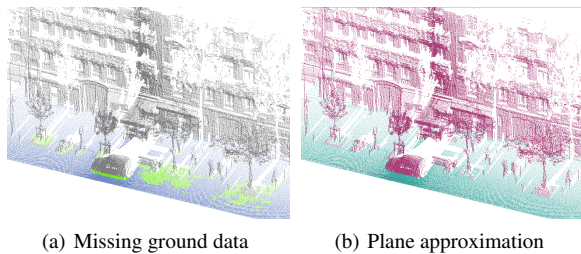

(a) Missing ground data   (b) Plane approximation

Figure 5: **(a)** Recovering missing ground points in green and**(b)** points that belong to the estimated plane in cyan.
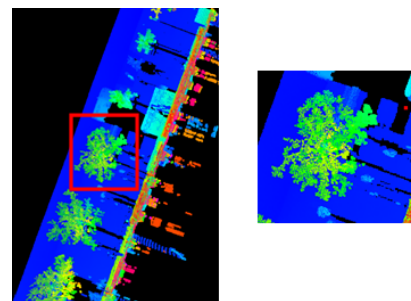
plane. Figure 5(b) shows the points that belong to the estimated plane.

Using the selected points we regenerate a new range image for pavement segmentation. Figure 6 shows a comparison between both range images. We can observe that points under the trees are recovered.
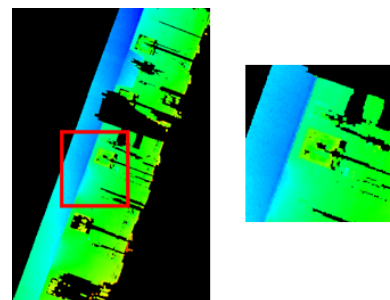
A block diagram of ground segmentation method and an example are given in Figure 7. First, in order to segment the pavement from ground data, a fine segmentation of range image is achieved. The segmentation method is based on the $\lambda-$ flat zones labeling algorithm introduced by Meyer in (Meyer, 1998).

Definition 1 *Two neighboring pixels p, q belong to the same quasi-flat zone of a function f, if their difference $|f_p - f_q|$ is smaller than or equal to a given λ value.*

$$\forall (p,q) \, neighbors : |f_p - f_q| \leq \lambda \qquad (3)$$

(a) Range image for artifact detection.

(b) Range image for pavement segmentation.

Figure 6: Range Images.

We want to obtain as few regions as possible, without merging the road and the pavement. Unfortunately in city planning, strict standards for pavement height do not exist. However, in the metropolitan areas the suggested heights are: $2[cm]$-pedestrian passage (handicap accessibility), $4[cm]$-vehicle access and $14[cm]$-pavement. As the height variations on the street level are small ($2[cm]$), a range image segmentation with a height $\lambda = 5[mm]$ will separately cluster pavement and road pixels into small regions, avoiding the leakage problem throughout a pedestrian access.

With this λ value the method produces a lot of small regions, because of the ground roughness. Hence, an area selection is carried out, by choosing regions larger than 50 pixels. Simultaneously, the range image gradient is calculated. The selected regions are used as markers and a constrained watershed by markers is carried out (Beucher and Meyer, 1993).

Once the segmentation is computed, a region adjacency graph RAG is obtained to represent this result. RAG representation
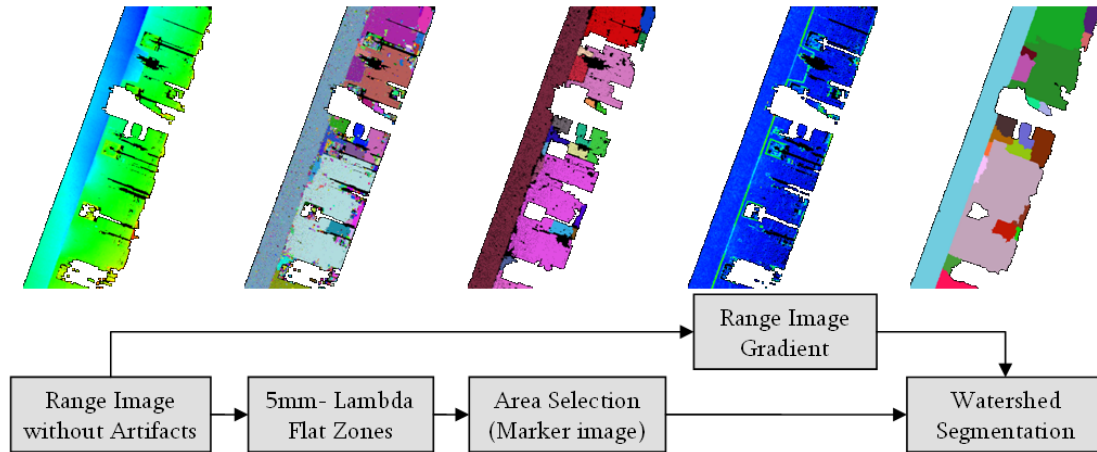
Figure 7: Diagram of pavement segmentation.

helps to select the border regions between the pavement and the road.

We denote RAG as $G = (R, E, W)$ where, $R = \{r_i\}$ is a partition into disjoint regions, $E = \{e_{ij} = r_i, r_j\}$ is the set of edges representing neighborhood relations. Each edge e_{ij} can be given a weight w_{ij}, providing a measure of dissimilarity between the two regions. In our case, w_{ij} is simply obtained by calculating the average contrast between local boundaries of thickness d (See Figure 8). The use of a local boundary increases the robustness against the pedestrian access and noisy points. After several tests, we chose $d = 5$. Edges with a valuation between $5[cm]$ and $18[cm]$ are selected as a boundary between the pavement and the road.
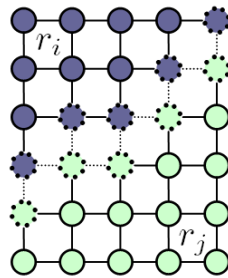

Figure 8: Local boundaries of thickness $d = 1$

Figure 9 shows RAG creation, local boundary to compute w_{ij} and contour extraction. An adequate delimitation of pavements and parking access is observed. The contour has been truncated due to an occlusion produced by a parked car. Our approach presents satisfactory results to detect city block pavements.
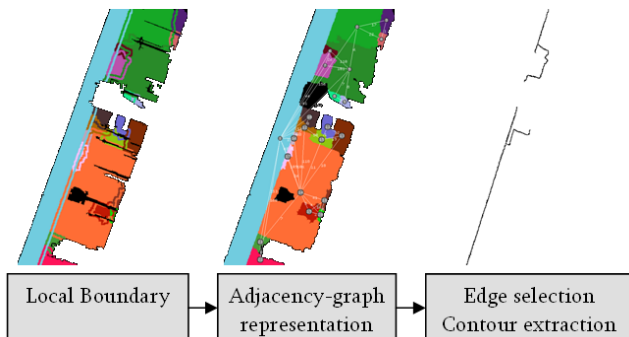

Figure 9: Diagram of region adjacency graph and contour selection.

5 CONCLUSIONS AND FUTURE WORK

A method of 3D point cloud analysis on street level urban environments has been presented. The analysis consists of two main parts: 1-filtering data in order to facilitate urban scene modeling (buildings, façades, roads and pavements) and 2-pavement segmentation to find the delimitation between pavements and roads. As a filtering of artifacts is applied on a top-view image, 3D projection may hide other artifacts under them (see Figure 4(a)). A 3D analysis of each artifact can be carried out, in order to separate them.

Pavement segmentation produces a contour image as a ground footprint. As a future work, we will work on image vectorization to allow ground modeling. The proposed method is robust to small noise points, because they are eliminated after selecting the largest regions of fine segmentation. As well, we handle with pedestrian access ($2[cm]$) thanks to the local boundary of the graph. However, if the pedestrian access height is lower than $2[cm]$, a pavement part can be merged with the road, missing this part in the segmentation and producing a wrong contour estimation.

The results obtained are satisfactory on the whole dataset. Extended tests on a larger database are foreseen in the framework of TerraNumerica project. Ongoing work includes analyzing color information, in order to improve artifact detection and pavement segmentation.

REFERENCES

Becker, S. and Haala, N., 2007. Combined feature extraction for façade reconstruction. In: ISPRS Workshop on Laser Scanning and SilviLaser, Espoo, Finland, pp. 44–50.

Beucher, S. and Meyer, F., 1993. The morphological approach to segmentation: the watershed transformation. In: E. R. Dougherty (ed.), Mathematical Morphology in Image Processing, Marcel Dekker, New York, chapter 12, pp. 433–481.

Boulaassal, H., Landes, T., Grussenmeyer, P. and Tarsha-Kurdi, F., 2007. Automatic segmentation of building facades using terrestrial laser data. ISPRS Workshop on Laser Scanning and SilviLaser, Espoo, Finland pp. 65–70.

Brostow, G. J., Shotton, J., Fauqueur, J. and Cipolla, R., 2008. Segmentation and recognition using structure from motion point

clouds. In: ECCV '08: Proceedings of the 10th European Conference on Computer Vision, Springer-Verlag, Berlin, Heidelberg, pp. 44–57.

Brun, X., Deschaud, J.-E. and Goulette, F., 2007. On-the-way city mobile mapping using laser range scanner and fisheye camera. In: 5th International Symposium on Mobile Mapping Technology (MMT' 07), Padova, Italy.

Dold, C. and Brenner, C., 2006. Registration of terrestrial laser scanning data using planar patches and image data. In: International Archives of Photogrammetry and Remote Sensing, pp. 25–27.

Foley, J. D., van Dam, A., Feiner, S. K. and Hughes, J. F., 1995. Computer Graphics: Principles and Practice in C. Second edn, Addison-Wesley Professional.

Goulette, F., Nashashibi, F., Ammoun, S. and Laurgeau, C., 2007. An integrated on-board laser range sensing system for on-the-way city and road modelling. Revue française de photogrammétrie et de télédétection 185, pp. 78.

Hernández, J. and Marcotegui, B., 2009. Point cloud segmentation towards urban ground modeling. In: 5th GRSS/ISPRS Joint workshop on remote sensing and data fusion over urban areas, Shangai, China.

Madhavan, R. and Hong, T., 2004. Robust detection and recognition of buildings in urban environments from ladar data. In: International Conference on Artificial Intelligence and Pattern Recognition, IEEE Computer Society, Los Alamitos, CA, USA, pp. 39–44.

Meyer, F., 1998. From connected operators to levelings. In: ISMM '98: Proceedings of the fourth International Symposium on Mathematical Morphology and its Applications to Image and Signal Processing, Kluwer Academic Publishers, Norwell, MA, USA, pp. 191–198.

Rottensteiner, F., 2003. Automatic generation of high-quality building models from lidar data. IEEE Computer Graphics and Applications 23(6), pp. 42–50.

Soille, P., 2003. Morphological Image Analysis: Principles and Applications. Springer-Verlag New York, Inc., Secaucus, NJ, USA.

Soille, P. and Gratin, C., 1994. An efficient algorithm for drainage networks extraction on DEMs. Journal of Visual Communication and Image Representation 5(2), pp. 181–189.

Stamos, I., Yu, G., Wolberg, G. and Zokai, S., 2006. 3d modeling using planar segments and mesh elements. In: International Symposium on 3D Data Processing, Visualization and Transmission, IEEE Computer Society, Washington, DC, USA, pp. 599–606.

Zhou, Q.-Y. and Neumann, U., 2008. Fast and extensible building modeling from airborne lidar data. In: GIS '08: Proceedings of the 16th ACM SIGSPATIAL international conference on Advances in geographic information systems, ACM, New York, NY, USA, pp. 1–8.